



HAL
open science

Flaw characterization in conductive media based on pulsed eddy current measurements: A fast non-iterative inversion approach

Roberto Miorelli, Anastassios Skarlatos, Christophe Reboud

► To cite this version:

Roberto Miorelli, Anastassios Skarlatos, Christophe Reboud. Flaw characterization in conductive media based on pulsed eddy current measurements: A fast non-iterative inversion approach. *IET Science Measurement and Technology*, 2021, 15 (3), pp.259-267. 10.1049/smt2.12027 . hal-04547788

HAL Id: hal-04547788

<https://hal.science/hal-04547788>

Submitted on 18 Apr 2024

HAL is a multi-disciplinary open access archive for the deposit and dissemination of scientific research documents, whether they are published or not. The documents may come from teaching and research institutions in France or abroad, or from public or private research centers.

L'archive ouverte pluridisciplinaire **HAL**, est destinée au dépôt et à la diffusion de documents scientifiques de niveau recherche, publiés ou non, émanant des établissements d'enseignement et de recherche français ou étrangers, des laboratoires publics ou privés.

Flaw characterization in conductive media based on pulsed Eddy current measurements: A fast non-iterative inversion approach

Roberto Miorelli  | Anastassios Skarlatos  | Christophe Reboud

CEA, List, Université Paris-Saclay, Palaiseau
F-91120, France

Correspondence

Anastassios Skarlatos, Université Paris-Saclay, CEA,
List, F-91120, Palaiseau, France.
Email: anastasios.skarlatos@cea.fr

Abstract

This paper proposes a non-iterative procedure for flaw(s) characterization based on Pulsed Eddy Current Testing (PECT) signals analysis. The adopted inversion strategy is based on the use of supervised statistical learning algorithms. A numerical forward solver, based on the Finite Integration Technique (FIT), is used for the generation of the training data (the input-targets couples of the learning algorithm). Predictions are then carried out in almost real-time using a non-linear kernel based regression method, known as kernel ridge regression. It turns out that the direct fit of the regression model to the raw PECT signals may lead to poor prediction accuracy due to the large cardinality of PECT signals. To remedy this problem, an adaptive sampling strategy has been adopted in this work. The performance of the proposed methodology is discussed and compared with solutions proposed in the literature.

1 | INTRODUCTION

Eddy-Current Testing (ECT) of conducting and/or ferromagnetic materials is primarily concerned with the detection and the dimensioning of structural anomalies like thinning, corrosion, appearance of fatigue cracks etc., before such defects become too critical for the integrity of the structure. Although simple defect geometries can be successfully addressed using relative simple techniques, such as amplitude and phase analysis of the eddy-current probe complex impedance under harmonic excitation, the interpretation of the inspection signals becomes difficult when complex geometries and defect shapes are involved. Typical situations of such complex signals are met during the inspection of riveted structures [1–4] or heat-exchanger tubes in the proximity of support plates [5, 6], the former consisting a significant problem for the aerospace industry and the latter been related with critical security issues in the nuclear plant maintenance.

Simple interpretation tools like the aforementioned complex plane analysis in such involved geometries can fail, and the use of more sophisticated inversion algorithms becomes a necessity. To provide an adequate amount of information to the inversion algorithm in order to minimise the inherit problem ill-posedness, one has to scan the area of interest and build contour plots of the respective probe response variations (in most cases

variations of the probe complex impedance), also known in ECT jargon as C-scans. The inverse mapping from these 2D scans to a set of defect characteristic parameters is then yielded by means of a cost-function minimization [7, 8].

A major drawback of classical iterative inversion approach discussed above is that thousands of calls of the forward solver are required in order to provide meaningful results. Thus, even if efficient dedicated solvers have been proposed in the past years in order to optimise the computation times, by decoupling the field calculation in the flawless structure and the defect response [4, 9–11], computational times remain non-negligible, especially when entire probe-scans need to be simulated. Thus the overall computation burden becomes prohibitive when complex situations like the aforementioned ones are targeted.

An additional difficulty is introduced when transient signals are considered, which is the case when dealing with Pulsed Eddy Current Testing (PECT) applications. The interest of using pulsed instead of harmonic excitation relies on the broadband content of the resulting signals, which, at least theoretically, can significantly increase the amount of the acquired information and hence to improve the performance of the characterization algorithm. The beneficial effect of using multiple frequency signals is demonstrated, for example, in [5, 6], where the additional information allows the separation of the defect signature from parasitic signals caused by geometrical irregularities such as the

This is an open access article under the terms of the [Creative Commons Attribution](https://creativecommons.org/licenses/by/4.0/) License, which permits use, distribution and reproduction in any medium, provided the original work is properly cited.

© 2021 The Authors. *IET Science, Measurement & Technology* published by John Wiley & Sons Ltd on behalf of The Institution of Engineering and Technology

tube support plates. This signal enhancement comes though at the price of increasing the number of calculations by a factor equal to the number of sampling points along the additional frequency/temporal dimension. This dimension corresponds to the number of frequencies, if the spectrum sampling and the inverse Fourier Transform is used to construct the time signals [12–16], the number of samples in the Laplace plane in case of calculation of the Laplace transformed response, [17] or the number of timesteps if the calculation is carried out directly in the time domain [18, 19].

In this context, Machine Learning (ML) algorithms [20, 21] can prove useful, in the sense that an expensive (rigorous) numerical solver is replaced by a so-called metamodel (also known as surrogate model), when massive evaluation is required. Hence, during a possibly expansive off-line phase, sets of inputs-targets couples are computed in order to obtain a so-called training set (sometimes called database). Thereupon, a kernel based regressor is fit on the training set in order to built an almost real-time estimator of the underlying numerical solver. This approach is referred to in the literature as supervised learning [20].

Very recently, the Machine Learning (ML) paradigm has been applied to perform non-iterative inversion studies based in ECT with promising results [22]. A hybrid approach combining the classical iterative minimization method based on a conjugate-gradient algorithm and an artificial neural network approach has been proposed for groove sizing using PECT signals [23].

A second issue that one has to encounter when dealing with PECT is the augmented dimension of the output space, resulting in a high cardinality of its elements. The direct consequence of this fact is that fitting the regression model directly on raw signals may lead to poor prediction accuracy or merely failure, when PECT signals are considered. In order to overcome this drawback, a dimensionality reduction method based on Principal Component Analysis (PCA) [24] is proposed in order to work directly in a reduced space of a much smaller dimension compared to the original (physical) space. This reduced space will be referred to in the context of this work as the extracted feature space. In this way, algorithms that can largely enhance the regression accuracy through wise sampling strategies can be developed.

This approach is followed in [16], where feature extraction is employed to address the classification problem. In this paper, a more general approach is devised in order to be able to tackle the inversion (regression in ML language) problem, and which is based on a generalization of ideas presented in [22, 25]. Since the input space of the physical problem parameters is replaced in this approach by the abstract feature space, the corresponding sampling strategy for the generation of the training set has to be modified accordingly in order to maximize the regression accuracy. Hence, provided a given budget of simulations, an adaptive generation of the training set by an homogeneous fill of the extracted feature space is proposed here. In this context, the main advances of this contribution of this article compared to the literature (e.g. [25–28]) consist in the development of an adaptive dataset generation algorithm aiming at:

- Enhancing the generation throughput thanks to the sampling strategy based on the projection of PECT data in the extracted features counterpart (e.g. adapt for parallel or distributed computing)
- Minimize the number of expensive-to-compute forward solver calls for inversion problems and increasing the regression performance through the use of vector-valued regressors algorithms
- Provide a general framework for dataset sampling strategies based on ECT signals (regardless of the technique employed)

The paper is structured as follows. In the next section, an outline of the Kernel Ridge Regression (KRR) approach with an outlook from the optimization problem perspective will be provided, followed by a brief introduction to the PCA algorithm. In Section 4.1, the proposed adaptive sampling algorithm will be described in detail and it will be applied for performing inversion tasks. In Section 5, numerical results will be presented and discussed. Some perspectives of this work are discussed upon at the end of the article together with concluding remarks.

2 | KERNEL RIDGE REGRESSION

In this section, we briefly introduce the solution of a non-linear regression problem by means of the kernel based regularized least square method, also known as Kernel Ridge Regression (KRR) [20, 29]. Let us define the input matrix $\mathbf{X} \in \mathbb{R}^{N \times D}$, where N stands for the number of samples and D for the dimension (cardinality) of the measurements. A set of targets is associated with every input, which is represented by the matrix $\mathbf{Y} \in \mathbb{R}^{N \times M}$, with M standing for the targets size. We define the dataset \mathbb{S} as a collection of inputs and targets such that $\mathbb{S} = \{(\mathbf{x}_1, \mathbf{y}_1), \dots, (\mathbf{x}_N, \mathbf{y}_N)\}$, where \mathbf{x}_n and \mathbf{y}_n represent the n^{th} row of matrices \mathbf{X} and \mathbf{Y} , respectively. The underlying idea in KRR, known in the literature as the kernel trick, relies on the introduction of a mapping between the input space \mathbf{X} and an alternative feature space with dimension F , in which the originally non-linear $\mathbf{X} - \mathbf{Y}$ relation is possibly transformed to a linear one [29, 30]. Thus, we shall define the mapping as follows

$$\phi : \mathbf{x} \in \mathbb{R}^{D \times 1} \mapsto \phi(\mathbf{x}) \in F \subseteq \mathbb{R}^{F \times 1}. \quad (1)$$

As a consequence, the mapped data set \mathbb{S} is described in the alternative feature space via $\mathbb{S}^* = \{(\phi(\mathbf{x}_1), \mathbf{y}_1), \dots, (\phi(\mathbf{x}_N), \mathbf{y}_N)\}$.

For the sake of notation clarity, we shall restrict ourselves to the case of scalar-valued targets, that is, $\mathbf{Y} \in \mathbb{R}^{N \times 1}$. The generalization to a vector valued data is straightforward. In the primal version, the KRR can be formulated as an optimization problem over the objective function $\mathcal{J}(\mathbf{w})$, such that [29, 30]

$$\mathbf{w} = \arg \min_{\mathbf{w}} \mathcal{J}(\mathbf{w}) = \arg \min_{\mathbf{w}} \sum_{n=1}^N (\mathbf{y}_n - g(\phi(\mathbf{x}_n)))^2 - \lambda \|\mathbf{w}\|^2, \quad (2)$$

where $\lambda \geq 0$ represents the regularization coefficient, and

$$g(\phi(\mathbf{x}_n)) = \langle \mathbf{w}, \phi(\mathbf{x}_n) \rangle = \mathbf{w}^\top \boldsymbol{\phi} = \sum_{d=1}^D w_d \phi(\mathbf{x}_{nd}), \quad (3)$$

is the linear prediction function associated with the mapped input $\phi(\mathbf{x}_n)$. The superscript \top stands for the transpose. By taking the gradient of $\mathcal{J}(\mathbf{w})$ with respect to \mathbf{w} and equating to zero, one obtains the primal solution as

$$\mathbf{w} = (\mathbf{K}\mathbf{K}^\top + \lambda \mathbf{I}_N)^{-1} \mathbf{K}^\top \mathbf{Y}, \quad \text{with } \mathbf{w} \in \mathbb{R}^{N \times 1}, \quad (4)$$

where \mathbf{K} represents the kernel matrix, which is a Gram matrix with entries given by

$$K_{ij} = \langle \phi(\mathbf{x}_i), \phi(\mathbf{x}_j) \rangle = \kappa(\mathbf{x}_i, \mathbf{x}_j), \quad (5)$$

and $\kappa(\mathbf{x}, \cdot)$ being the kernel function used to evaluate the inner product $\langle \cdot, \cdot \rangle$ in the feature space mapped by $\phi(\cdot)$. In the machine learning community, (5) is also known under the name of kernel trick or kernel substitution. The kernel trick allows to work directly in the feature space by considering the original space \mathbf{X} without explicitly performing the mapping (1) in (2) [29, 31]. Notice here that the solution of (4) can become computationally demanding when the size of the feature space F is much larger than D . That is, a system of equation with a matrix of size $F \times F$ needs to be solved. Alternatively, the dual representation of (2) can be obtained by expressing (4) as [20, 29, 31]

$$\mathbf{w} = \sum_{n=1}^N \alpha_n \phi(\mathbf{x}_n) = \boldsymbol{\Phi}^\top \boldsymbol{\alpha}, \quad (6)$$

with

$$\alpha_n = \lambda^{-1} \{ \mathbf{w}^\top \phi(\mathbf{x}_n) - Y_n \}, \quad \text{with } \boldsymbol{\alpha} \in \mathbb{R}^{N \times 1}. \quad (7)$$

Then by replacing (6) into (2), one can show that the dual formulation is obtained as [29, 30]

$$\begin{aligned} \boldsymbol{\alpha} &= \arg \max_{\boldsymbol{\alpha}} \mathcal{J}(\boldsymbol{\alpha}, \lambda, S) \\ &= \arg \max_{\boldsymbol{\alpha}} \{ \boldsymbol{\alpha}^\top \mathbf{K}\mathbf{K}\boldsymbol{\alpha} - \boldsymbol{\alpha}^\top \mathbf{K}\mathbf{Y} + \mathbf{Y}^\top \mathbf{Y} + \lambda \boldsymbol{\alpha}^\top \mathbf{K}\boldsymbol{\alpha} \}. \end{aligned} \quad (8)$$

By taking the gradient of $\mathcal{J}(\boldsymbol{\alpha})$ with respect to $\boldsymbol{\alpha}$ and equating to zero, the solution is obtained as

$$\boldsymbol{\alpha} = (\mathbf{K} + \lambda \mathbf{I}_N)^{-1} \mathbf{Y}. \quad (9)$$

In other words, passing to the dual formulation, we need to invert an $N \times N$ matrix in order to get $\boldsymbol{\alpha}$, which is computationally much less expensive than inverting the $F \times F$ matrix of the primal solution. Once $\boldsymbol{\alpha}$ is calculated through (9), the regression is applied on a set made by T samples (i.e. the test set \mathbf{X}^{tst})

through

$$\begin{aligned} g(\mathbf{X}^{\text{tst}}) &= \boldsymbol{\alpha}^\top \mathbf{K}(\mathbf{X}, \mathbf{X}^{\text{tst}}) \\ &= \mathbf{Y}^\top (\mathbf{K}(\mathbf{X}, \mathbf{X}^{\text{tst}}) + \lambda \mathbf{I}_N)^{-1} \mathbf{k}(\mathbf{X}^{\text{tst}}), \end{aligned} \quad (10)$$

with $\mathbf{X}^{\text{tst}} \in \mathbb{R}^{T \times D}$ and $K_j(\mathbf{X}_j^{\text{tst}}) = [\kappa(\mathbf{x}_j^{\text{tst}}, \mathbf{x}_1), \dots, \kappa(\mathbf{x}_j^{\text{tst}}, \mathbf{x}_N)]^\top$.

3 | DIMENSIONALITY REDUCTION BY PROJECTION ONTO PRINCIPAL COMPONENTS

The number of considered dimensions of D may be detrimental to the learning task, reducing both accuracy and computational efficiency of the regression process. This phenomenon is known in machine learning under the name of "curse of dimensionality". When PECT signals are simulated and/or measured over linear or surface scans, one may be confronted with $D \geq 10^4$. In fact, to each probe position, hundreds of time samples are collected, thus a strategy to extract a meaningful subset of features is needed. That is, we must, in such cases, project the NdT signals onto an intrinsic or latent space of a typically lower or much lower dimension than the original space.

In this paper, the Principal Component Analysis (PCA) [24], also known under the name (Karhunen–Loeve transform), has been selected as a feature extraction method. Provided a set of inputs $\mathbf{x}_n \in \mathbb{R}^{1 \times D}$ with $n = 1, \dots, N$, that is supposed to have zero-mean, PCA provides a subspace of dimension $J \leq D$ such that the projection of \mathbf{x}_n on the subspace spanned by J maximizes the variance of the data [24]. Thus the extracted feature space is described by a set of mutually orthogonal vectors J . These vectors are known as principal components/axes. From the computational point of view, PCA can be efficiently performed by employing Singular Value Decomposition (SVD) of the covariance matrix associated with the dataset inputs $\mathbf{X} \in \mathbb{R}^{N \times D}$ [20]. For the dimensionality reduction stage through PCA, we first built the covariance matrix $\boldsymbol{\Sigma} = \mathbf{X}^\top \mathbf{X}$, then we decompose $\boldsymbol{\Sigma}$ through SVD as

$$\boldsymbol{\Sigma} = \mathbf{U}\mathbf{D}\mathbf{V}^\top, \quad (11)$$

where $\mathbf{U} \in \mathbb{R}^{D \times D}$ $\mathbf{V} \in \mathbb{R}^{D \times D}$ are the matrices containing the eigenvectors. $\mathbf{D} \in \mathbb{R}^{N \times N}$ is the diagonal matrix of the singular values that, for the sake of simplicity, we assume it being ordered in decreasing amplitude. When applying the PCA, we are interested in keeping only a subset of the greatest J eigenvalues, which implies the projection matrix $\mathbf{U} \in \mathbb{R}^{N \times J}$. Formally speaking, \mathbf{U} has rank equal to J , and hence it maps the original space to the new extracted feature space of $J \times N$ dimensions. The number of latent components J can be conveniently chosen by considering the cumulative sum of the ratio between the first n eigenvalues of \mathbf{D} and their sum over N , that is, by considering the so-called explained variance. In the limit case, where the explained variance of the entire dataset is accounted,

the extracted subspace coincides with the original one, that is, $J = D$.

4 | TRAINING SET GENERATION AND PREDICTIONS IN THE EXTRACTED FEATURE SPACE

4.1 | Training set generation by adaptively filling the extracted feature space

Unlike other PCA-based strategies already studied in the literature (e.g. [16]), here an ad-hoc training set generation has been applied for carrying out non-iterative inversion. Given the significant computational time per direct solver call, the purpose of this stage is to obtain a training set, which, for a predefined simulations budget, maximizes therein contained information. Furthermore, in contrast to the classification tasks addressed in [16], the problem targeted hereafter is the construction of an automatic quantitative and robust inversion strategy based on machine learning regression (i.e. KRR).

In recent years, several efforts have been devoted in the design of advanced training set generation schemata. Training set sampling strategies can be divided into two main families: the input space filling [32, 33], which aims to fill homogeneously the parameter space, and the adaptive space sampling, which selects the samples from a subset satisfying a given objective function [22, 25–27]. In this work, we propose a sampling strategy relying on sampling the space spanned by the extracted feature space, which we refer to as Feature Space Filling (FSF) algorithm. It is worth mentioning that a similar procedure has already been studied in the framework of partial least squares feature extraction [22]. In contrast with that work, the approach proposed here relies to PCA, and it aims to generate—that is, fill—the extracted feature space without performing any iterative loop with an obvious gain in terms of computational efficiency since it is suitable for parallel computation on clusters or GPU. Furthermore, the proposed schema can be readily applied to any other, linear or non-linear, dimensionality reduction method regardless of the knowledge of the targets (i.e. in an unsupervised way).

The FSF algorithm is based on three main steps. First, a set of I points is chosen in order to provide a suitable initialization through standard design of experiments approach, like a coarse tensor grid or pseudo-random strategies (e.g. Latin Hypercube Sampling (LHS), Sobol's or Halton's sequences etc.). Then, the forward solver (\mathcal{F}) is called on the $\mathbf{Y}^{init} \in \mathbb{R}^{I \times M}$ sampling points providing the associated $\mathbf{X}^{init} \in \mathbb{R}^{I \times D}$ signals and hence the initialization dataset $\mathbb{S}^{init} = \{(\mathbf{x}_1, \mathbf{y}_1), \dots, (\mathbf{x}_I, \mathbf{y}_I)\}$ is constituted. Thereupon, the reduced space is determined through PCA leading to the dimensionality reduced initialization dataset $\tilde{\mathbb{S}}^{init} = \{(\tilde{\mathbf{x}}_1, \mathbf{y}_1), \dots, (\tilde{\mathbf{x}}_I, \mathbf{y}_I)\}$, where tilde refers to the projected vectors. We have discussed in Section 3 that the principal component space can be seen as the space that maximizes the variance of the considered signals set. In this framework, a homogeneous fill of the space spanned by the principal components corresponds in capturing the variance of all the signals associated to the con-

sidered problem. For the selection of model evaluations during the feature space filling, the KRR, outlined in Section 2, is fitted to the initialization set $\mathbb{S}_{fwd}^{init} = \{(\mathbf{y}_1, \tilde{\mathbf{x}}_1), \dots, (\mathbf{y}_I, \tilde{\mathbf{x}}_I)\}$, where the subscript "fwd" refers to forward relationship. Then, (10) is applied on $\mathbf{Y}^{trial} \in \mathbb{R}^{T \times M}$ to predict the eigenvalues components into the extracted feature space providing $\tilde{\mathbf{x}}^{trial} \in \mathbb{R}^{T \times J}$, where T is a representative (large) set of target candidates. Due to the excessive computational burden for the simulation of the whole set of candidate samples, an add-and-sorting procedure aiming at maximizing the information content (i.e. the variance) is applied. More precisely, the procedure consists of iteratively adding a candidate sample when the corresponding position in the feature space is "sufficiently far" from the features of the rest of the samples. In the opposite case, the sample is discarded. This criterion is formally expressed by (12) with the term "sufficiently far" being translated to a minimum distance value in the feature space. The iterations are terminated when the predefined number of samples C has been reached, yielding the sought training set $\tilde{\mathbb{S}} = \{(\tilde{\mathbf{x}}_1, \mathbf{y}_1), \dots, (\tilde{\mathbf{x}}_N, \mathbf{y}_N)\}$.

$$\left\| \text{PCA} [g(\mathbf{Y}^{trial})] - \text{PCA} [\mathcal{F}(\mathbf{Y}^{init})] \right\|^2 > tol, \quad (12)$$

where $\text{PCA}[\cdot]$ indicates the projection of the dataset $[\cdot]$ onto the space spanned by the principal components according to (11). On the right hand side of (12), tol refers to a tolerance which can be properly chosen as a ratio of the mean distances between points in the feature space. In this work, we have chosen a tolerance value equal to $tol = \text{mean}(\text{median}(\|\text{PCA}[\mathcal{F}(\mathbf{Y}^{init})]\|^2))$. The FSF algorithm is provided in the form of a pseudo-code in Algorithm 1.

4.2 | Learning the inverse model and perform prediction in the reduced space

Let $\tilde{\mathbb{S}} = \{(\tilde{\mathbf{x}}_1, \mathbf{y}_1), \dots, (\tilde{\mathbf{x}}_N, \mathbf{y}_N)\}$ be the dataset obtained via the FSF Algorithm 1. The learning procedure presented herein consists of fitting the KRR, presented in Section 2, to $\tilde{\mathbb{S}}$. The applied kernel function, introduced in (5), is the so-called Gaussian kernel (also known under the name of radial basis function kernel), and it is defined as

$$k(\mathbf{x}_i, \mathbf{x}_j) = \exp \left(-\frac{\|\tilde{\mathbf{x}}_i - \tilde{\mathbf{x}}_j\|}{2\sigma} \right). \quad (13)$$

In order to properly fit the KRR model to the data, a cross-validation technique [29] has been applied to tune σ and the regularization coefficient λ in (7). This step is known in ML as training phase.

Once the model has been fitted, data regression can be achieved at almost real time by applying (10). Let $\mathbf{X}^{tsf} \in \mathbb{R}^{T \times D}$ be the matrix representing a new set of $T \times D$ points (e.g. the set of PECT signals sampled in space and time), from which we wish to predict $T \times M$ parameters (in case of NdT applications, a the parameters of the flaw) defined as $\mathbf{Y}^{pred} \in \mathbb{R}^{T \times M}$. Since KRR has been trained on the projected data (13), one needs to project the test set onto the latent feature space before the prediction evaluation in the following fashion

ALGORITHM 1 FSF sampling strategy

Begin

initialize the training set with I samples:

$$\mathcal{S}^{init} = \{(\mathbf{x}_1, \mathbf{y}_1), \dots, (\mathbf{x}_I, \mathbf{y}_I)\}$$

project the data onto the extracted feature space spanned by the first J principal components:

$$\tilde{\mathcal{S}}^{init} = \{(\tilde{\mathbf{x}}_1, \mathbf{y}_1), \dots, (\tilde{\mathbf{x}}_I, \mathbf{y}_I)\}$$

fit KRR model $f(\tilde{\mathcal{S}}^{init}_{jwd})$ (see Equation 7) to the dataset:

$$\tilde{\mathcal{S}}^{init}_{jwd} = \{(\mathbf{y}_1, \tilde{\mathbf{x}}_1), \dots, (\mathbf{y}_I, \tilde{\mathbf{x}}_I)\}$$

generate a set of T candidates via pseudo-random sequences:

$$\mathbf{Y}^{trial} = LHS(T, M)$$

perform predictions through KRR model ($f(\cdot)$) based on the $\mathbf{Y}^{trial} \in \mathbb{R}^{T \times M}$:

$$\tilde{\mathbf{X}}^{trial} = f(\mathbf{Y}^{trial}) \text{ with } \in \mathbb{R}^{T \times J}$$

add the first C candidates that fulfill the distance criteria:

$$\mathbf{X}_1^{candid} = []; \mathbf{Y}_1^{candid} = []$$

for $t = 1$ to T do

if $c > C$ then

break

else

check if the distance between extracted components among the candidate sample and the already added samples is fulfilled:

$$\text{if } \|\text{PCA}[\mathcal{E}(\mathbf{Y}_t^{trial})] - [\tilde{\mathbf{X}}^{init}, \tilde{\mathbf{X}}^{candid}]\|^2 > tol \text{ then}$$

update the parameter space:

$$\mathbf{Y}^{candid} = [\mathbf{Y}_{1, \dots, c-1}^{trial}, \mathbf{Y}_c^{trial}]$$

update the extracted feature space:

$$\tilde{\mathbf{X}}^{candid} = [\tilde{\mathbf{X}}_{1, \dots, c-1}^{candid}, \tilde{\mathbf{X}}_c^{candid}]$$

$$c = c + 1$$

end if

$$t = t + 1$$

end if

end for

call the forward solver on the C retained candidates and update the training set:

$$\tilde{\mathbf{X}}^{new} = \text{PCA}[\mathcal{F}(\mathbf{Y}^{candid})] \text{ with } \in \mathbb{R}^{C \times J}$$

fill the final training set containing samples:

$$\mathcal{S} = \{(\tilde{\mathbf{x}}_1, \mathbf{y}_1), \dots, (\tilde{\mathbf{x}}_I, \mathbf{y}_I)\} \cup \{(\tilde{\mathbf{x}}_{I+1}, \mathbf{y}_{I+1}), \dots, (\tilde{\mathbf{x}}_{I+C}, \mathbf{y}_{I+C})\} = \{(\tilde{\mathbf{x}}_1, \mathbf{y}_1), \dots, (\tilde{\mathbf{x}}_N, \mathbf{y}_N)\}$$

End

$$\tilde{\mathbf{X}}^{tst} = \mathbf{X}^{tst} \mathbf{U}, \quad \text{with } \tilde{\mathbf{X}}^{tst} \in \mathbb{R}^{T \times J}, \quad (14)$$

where $\mathbf{U} \in \mathbb{R}^{D \times J}$ has been obtained from the training set through PCA algorithm outlined in Section 3 based on the knowledge of \mathbf{X} .

5 | APPLICATION TO THE CHARACTERIZATION OF DEFECTS

5.1 | Definition of the problem addressed

The above presented algorithm is applied for the detection and the dimensioning of small cracks in steam generator tubes, which are lying in the proximity of ferromagnetic tube support

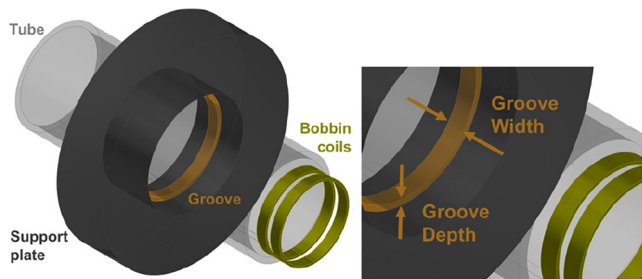


FIGURE 1 Sketch of the considered inspection problem with details associated with the groove parameters

plates with cylindrical openings. The measurement signals are variations of an Eddy current probe response, as the latter interacts with magnetic field anomalies, due to the presence of cracks or other material anomalies. The sensing probe consists, in this particular case, of a number of air-cored coils, and it moves along the interior of the tube. This is an important nuclear safety problem, where the purpose is to detect and characterise steam generator tube degradations, which may potentially lead to water coolant leakage from the primary to the secondary coolant circuit thus provoking a contamination incident.

The presence of large conducting/ferromagnetic pieces in the vicinity of the steam generator tube, like steel support plates, increases the complexity of the crack detection due to the strong interaction of these parts with the Eddy current probe, which alter and may even completely mask the crack signature [5, 6]. Thus, in order to be able to separate the eventual crack signal from the rest of the contributions, an increase in the amount of acquired information is required. The standard way to enhance the signal information is via combination of measurements acquired at different frequencies [5]. The main idea in this technique is to form a weighted sum of the signals obtained at different frequencies in order to eliminate the signature of the plate. In a recent contribution, the use of classifiers based on ML approaches has been proposed for the detection of defects in the proximity of external structures like support plates and material deposits with promising results [34].

PECT inspection is inherently broadband, which makes it a good candidate for the improvement of the crack signature extraction in environments consisting of various perturbation components. In this context, ML-based approaches using transient signals, as the approach of the present contribution, can provide an interesting framework for addressing the problem of crack detection and dimensioning in the vicinity of external structures.

In this section, we present the numerical results obtained for the inversion of PECT crack signals in the vicinity of a support plate (see Figure 1), and we study the performance of the proposed algorithm in terms of prediction accuracy and robustness to Additive White Gaussian Noise (AWGN) corruption. A non-magnetic conductive tube with conductivity equal to 1.0 MS/m and inner and outer radius equal to 17.96 mm and 19.05 mm, respectively, is affected on the outer side by a 2D axis symmetric groove just beneath the support plate. The support plate is modelled as a thick ferromagnetic external tube wall with inner

and outer radius equal to 11.30 mm and 20.00 mm, respectively, and thickness equal to 19.00 mm. The support plate conductivity is 3.0 MS/m, and its relative permeability is equal to 50. The probe consists of two axial coils connected in differential mode, and it moves along the tube axis. The coils inner radius is equal to 7.83 mm, the outer radius is 9.25 mm, and its length is 2.0 mm. The two coils are wound with 70 each, and they are separated by a 2.0 mm gap. The excitation signal injected into the emitting coil is an increasing exponential with time constant $\tau = 15$ ms and duration of $T = 25.0$ ms, and the current amplitude at its peak is equal to 1 A.

5.2 | Definition and details on the numerical simulation campaign

The training set is obtained via the FSF algorithm, which has been initialized with 100 samples generated in a Latin hypercube sampling. The considered parameters range is equal to $[0.8, 1.0]$ mm and $[1.1, 2.0]$ mm for groove depth and width, respectively. Thus, 100 samples have been selected through FSF schema and added to the initialization in order to built the final training set. The axial scan comprises four sampling points equally distributed with a step of 3.0 mm between them. The temporal signals have been discretised using 100 time samples.

Hence, the training set are 2D signals, whose first axis corresponds to an axial scan of four points, whereas the second dimension stands for a temporal discretization with 100 timesteps associated to the axial and the radial components of the magnetic flux density variation. The above sampling scheme results in a training set size with $\mathbf{X} \in \mathbb{R}^{200 \times 800}$ PECT raw signals generated by accounting $\mathbf{Y} \in \mathbb{R}^{200 \times 2}$ inputs.

When visualizing the samples distribution in the groove parameter space, we can notice that there is a clear tendency of FSF to sample the deepest and widest groove values. This is coherent with the FSF sample strategy since these zones are the ones responsible for the strongest variations which is where the highest values of the variance are to be found. Looking at Figure 2(b), we can notice that the initialization procedure tends to create clusters of samples that cannot capture the variance of the data since “holes” appear in the project feature space. On the other hand, the FSF sampling tends to fill the gap between the initialization samples in an almost homogeneous fashion.

In this paper, we have chosen to apply a KRR based on Gaussian kernel, thus both the regularization parameter λ and the kernel parameter σ have been tuned via a fivefold cross validation procedure [22, 29]. The sampling intervals for α and γ parameters are $[10^2, 10^{-11}]$ and $[10^{-8}, 10^7]$, respectively, with logarithmic discretization. Figure 3(a) and (b) shows the inversion results obtained by an unknown test set with 200 samples. The training set was generated by randomly applying the FSF training set generation and keeping only the first three principal components, which correspond to 99% of the explained variance. In Figure 3(c) and (d), the prediction results are shown for a training set generated via LHS design counting 200 samples without applying PCA dimensionality reduction. Observing the

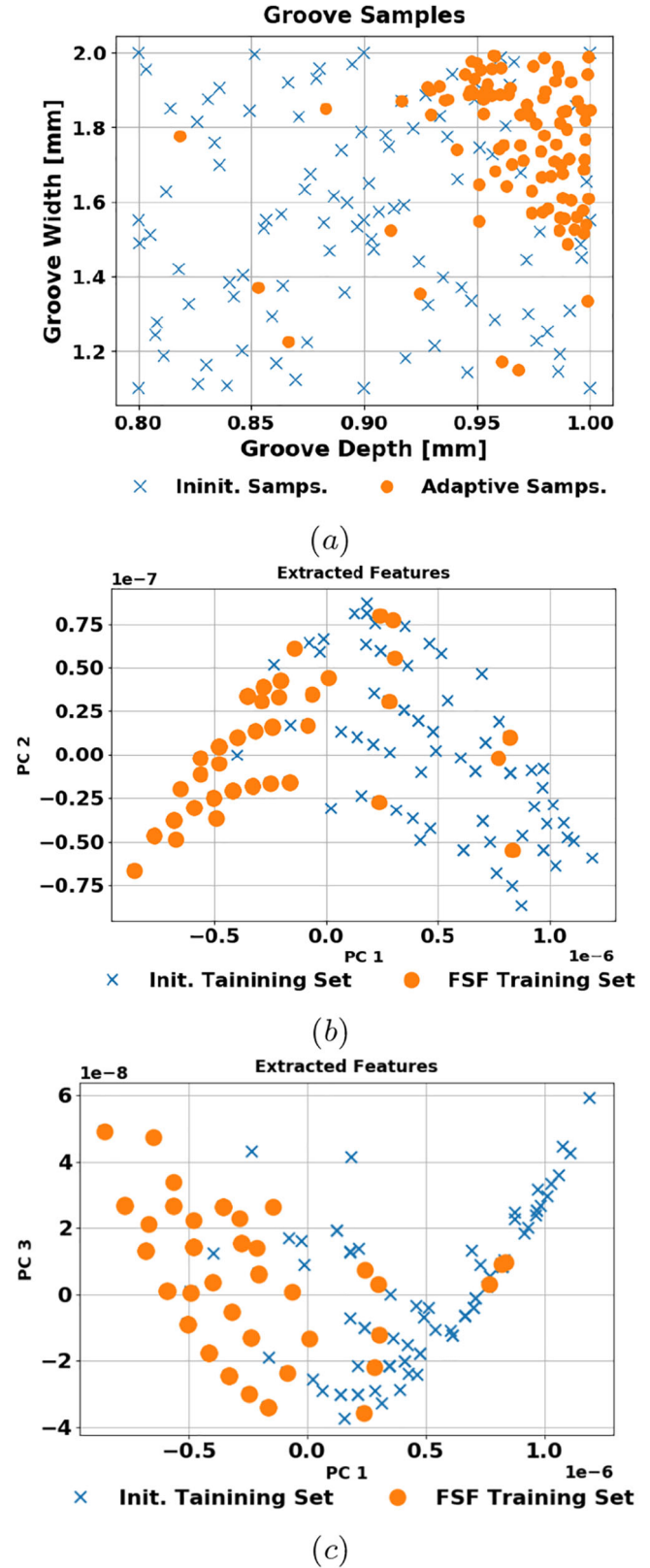


FIGURE 2 “x”: initialization points, “•”: FSF points. (a) Groove parameters compounding the training set and simulated through the numerical solver. (b) 2D scatter plot collecting the first and the second principal components (PCs). (c) First and third principal components.

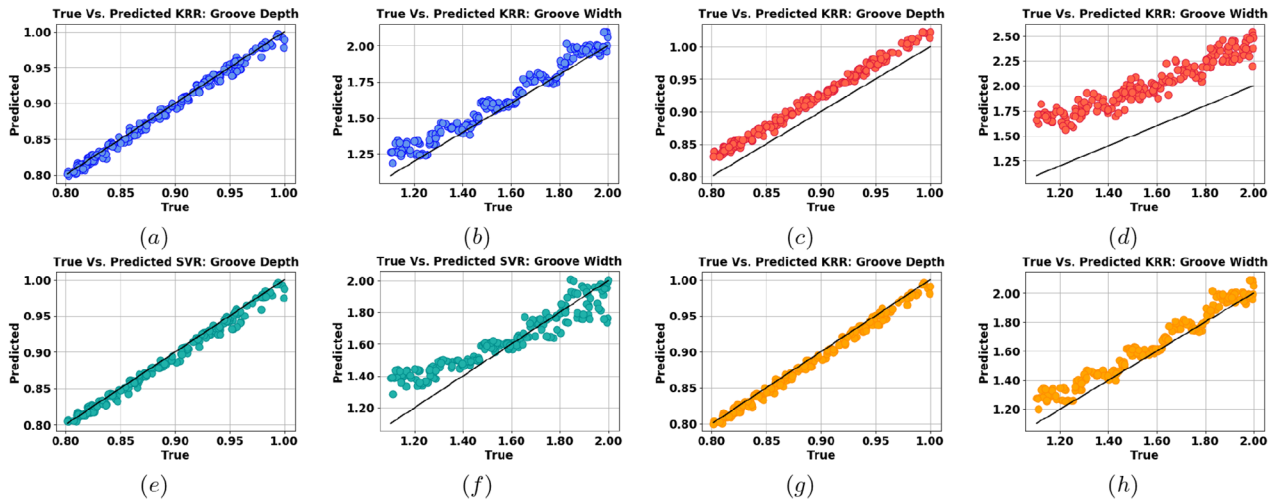


FIGURE 3 True versus predicted plots obtained by performing predictions on a synthetic noised test set with SNR = 20 dB, considering both groove depth and width. In (a) and (b), FSF was used with three principal components. In (c) and (d), no dimensionality reduction was used. (e), (f) and (g) and (h) present results obtained with sampling proposed in [22].

above-mentioned couple of figures, concerning the groove width, one can notice that performance is improved when FSF with dimensionality reduction is employed since results are more aligned and less spread along the 45° solid line representing the perfect agreement between experiments and predictions. These results show that learning a model accounting the three dimensions (the ones associated to PCA feature extraction) leads to overall better performance than considering the whole PECT signal.

Furthermore, looking at Figure 2, one can readily notice that the mapping between parameter space (i.e. Figure 2(a)) and extracted PCA components (i.e. Figure 2(b) and (c)) is not trivial since it involves a non-linear regression task. That is, one cannot easily infer the groove size by analysing the groove parameter space and PCA space separately.

5.3 | Obtained results analysis and discussion

In Figure 3(e)–(h), we show the results obtained by applying the adaptive sampling strategy proposed in [22]. Compared to FSF (i.e. Figure 3(a) and (b)) one can notice that slightly worst results are obtained by the approach [22] either considering Support Vector Regressor (SVR) model (Figure 3(e) and (f)) or KRR model (Figure 3(g) and (h)) applied on the same adaptively generated training set.

Performing a closer analysis on the different group of plots in Figure 3, we can notice that inversion based on complete PECT signals leads to poor results for both the parameters considered (i.e. Figure 3(c) and (d)). This is due to the high cardinality of PECT signals (tenth of hundreds of samples in time), such behaviour is also known as curse of dimensionality issue. Furthermore, Figure 3(e) and (f) show that the regression strategy used in [22] provide much worst results in predicting the smaller values of the groove width. This is very likely due to the use of scalar-valued SVR regressor [22]. On the other hand, in Figure 3(g) and (h), one can notice that the vector-valued

KRR regressor is able to enhance the inversion accuracy once the sampling schema in [22] is employed. That is, as shown in Figure 4, one can notice that the robustness of the FSF sampling strategy, compared to [22] regardless of the regressor used, is clearly superior for SNRs smaller than 20 dB. Furthermore, it is worth mentioning that, unlike [22], the sampling technique studied in this paper enables a more CPU time efficient training set generation (e.g. multiprocessing, distribute calculations etc.) since no cross-validation is needed on the choice of the principal components (i.e. explained variance is chosen once based on statistical reasoning).

It worth mentioning that in order to carry out the whole set of 100 inversions, KRR required about 0.02 s on a standard laptop (e.g. Dell Precision 5520 equipped with Intel Xeon E3-1505M v6).

6 | CONCLUSION AND PERSPECTIVES

This paper proposes a training set generation strategy based on adaptive sampling of PCA feature space, which is then used to train a kernel ridge regressor targeting non-iterative parametric inversion for crack characterization based on PECT signals. The performed analysis demonstrates the accuracy improvement of the inversion results, when FSF sampling is applied via projection of data onto the principal components subspace in combination with a KRR, with respect to non-adaptive strategies. Furthermore, a marginal improvement in terms of accuracy and a robustness enhancement against AWGN corruption has been obtained via application of the FSF sampling compared to the adaptive sampling method [22].

Even not explicitly underlined in the paper, the FSF approach can be also employed for the construction of training sets in view of non-iterative predictions in the forward sense (i.e. meta-models). In the latter case, one should replace the last step in Algorithm 1 with $\mathcal{S}^{final} = \{(\mathbf{y}_1, \tilde{\mathbf{x}}_1), \dots, (\mathbf{y}_N, \tilde{\mathbf{x}}_N)\}$ and train the KRR consequently. It must be also stressed out that the FSF

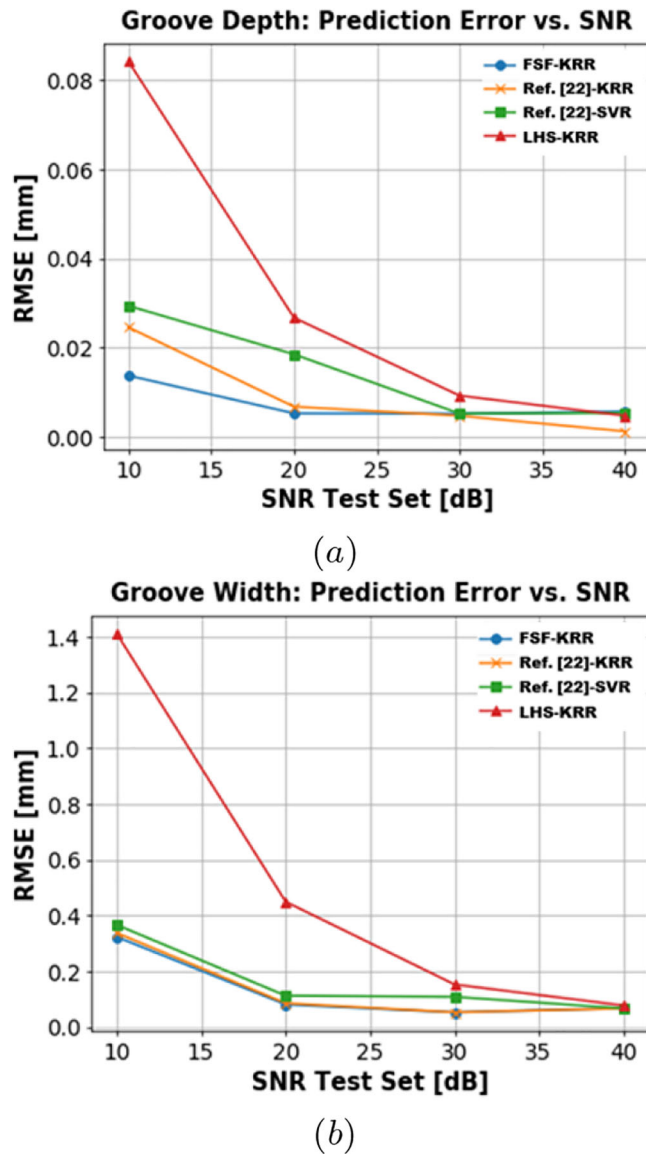


FIGURE 4 Regression results accuracy versus different AWGN levels imposed on the test set. The Root Mean Square Error (RSME) is shown for FSF, Lating hypercube sampling (LHS), and [22] (with SVR and KRR regressors) sampling strategies for groove (a) depth and (b) width, respectively.

strategy does not depend to the kernel-based method employed, and it can be extended directly to other linear and non-linear feature extraction methods [35].

ORCID

Roberto Miorelli  <https://orcid.org/0000-0003-3728-2227>

Anastassios Skarlatos  <https://orcid.org/0000-0001-5589-5145>

REFERENCES

- Knopp, J.S., et al.: Numerical and experimental study of eddy current crack detection around fasteners in multi-layer structures. In: Thompson, D.O., Chimenti, D.E. (eds.) *Review of Progress in Quantitative Nondestructive Evaluation*, vol. 23, pp. 336–343. American Institute of Physics, New York (2004)
- Knopp, J.S., et al.: Considerations in the validation and application of models for eddy current inspection of cracks around fastener holes. *J. Nondestruct. Eval.* 25(3), 123–137 (2006)
- Knopp, J.S., et al.: Computational methods in eddy current crack detection at fastener sites in multi-layer structures. *Nondestruct. Test. Eval.* 24(1–2), 103–120 (2009)
- Pipis, K., et al.: ECT-signal calculation of cracks near fastener holes using an integral equation formalism with dedicated Green's kernel. *IEEE Trans. Magn.* 52(4), 6200608 (2016)
- Skarlatos, A., et al.: Modeling of steam generator tubes inspection in the proximity of support plate's area via a coupled finite element - Volume integral method approach. In: Shin, Y.K., Lee, H.B., Song, S.J. (eds.) *Studies in Applied Electromagnetics and Mechanics*, vol. 32, pp. 51–58. IOS Press, Amsterdam (2009)
- Skarlatos, A., et al.: Eddy current inspection of steam generator tubes near support plates with trefoil and quatrefoil-shaped holes: a hybrid volume integral - finite elements approach. In: Knopp, J., Blodgett, M., Wincheski, B., Bowler, N. (eds.) *Studies in Applied Electromagnetics and Mechanics*, vol. 33, pp. 26–33. IOS Press, Amsterdam (2010)
- Bowler, J.R.: Eddy-current interaction with an ideal crack. II. The inverse problem. *J. Appl. Phys.* 75(12), 8138–8144 (1994)
- Abubakar, A., van den Berg, P.M.: Iterative forward and inverse algorithms based on domain integral equations for three-dimensional electric and magnetic objects. *J. Comput. Phys.* 195, 236–262 (2004)
- Skarlatos, A., et al.: Electromagnetic modeling of a damaged ferromagnetic metal tube by a volume integral equation formulation. *IEEE Trans. Magn.* 44, 623–632 (2008)
- Bowler, J.R., et al.: Eddy current probe signals due to a crack at a right-angled corner. *IEEE Trans. Magn.* 48(12), 4735–4746 (2012)
- Miorelli, R., et al.: Efficient modeling of ECT signals for realistic cracks in layered half-space. *IEEE Trans. Magn.* 49(6), 2886–2892 (2013)
- Theodoulidis, T., et al.: Extension of a model for eddy current inspection of cracks to pulsed excitations. *NDT & E Int.* 47, 144–149 (2012)
- Xie, S., et al.: Efficient numerical solver for simulation of pulsed eddy current testing signals. *IEEE Trans. Magn.* 47(11), 4582–4591 (2011)
- Xie, S., et al.: Development of a very fast simulator for pulsed eddy current testing signals of local wall thinning. *NDT & E Int.* 51, 45–50 (2012)
- Li, Y., et al.: Fast analytical modelling for pulsed eddy current evaluation. *NDT & E Int.* 41, 477–483 (2008)
- Chen, T., et al.: Feature extraction and selection for defect classification of pulsed eddy current NDT. *NDT & E Int.* 41, 464–476 (2008)
- Theodoulidis, T., Skarlatos, A.: Efficient calculation of transient eddy current response from multilayer cylindrical conductive media. *Phil. Trans. R. Soc. A* 378, 20190588 (2020)
- Clemens, M., Weiland, T.: Transient eddy-current calculation with the FI-method. *IEEE Trans. Magn.* 35(3), 1163–1166 (1999)
- Dutiné, J., et al.: Explicit time integration of transient eddy current problems. *Int. J. Numer. Modell.*, 2017, pp. jnm.2227–n/a
- Theodoridis, S.: *Machine Learning: A Bayesian and Optimization Perspective*, 1st edn. Academic Press, London (2015)
- Miorelli, R., et al.: Database generation and exploitation for efficient and intensive simulation studies. *AIP Conf. Proc.* 1706(1), 180002 (2016). <https://aip.scitation.org/doi/abs/10.1063/1.4940632>
- Salucci, M., et al.: Real-time NDT-NDE through an innovative adaptive partial least squares SVR inversion approach. *IEEE Trans. Geosci. Remote Sens.* 54(11), 6818–6832 (2016)
- Xie, S., et al.: Sizing of wall thinning defects using pulsed eddy current testing signals based on a hybrid inverse analysis method. *IEEE Trans. Magn.* 49(5), 1653–1656 (2013)
- Jolliffe, I.T.: *Principal component analysis*. Springer Series in Statistics. Springer-Verlag, New York (1986).
- Bilicz, S., et al.: Kriging-based generation of optimal databases as forward and inverse surrogate models. *Inverse Probl.* 26(7), 074012 (2010)
- Forrester, A.I.J., Keane, A.J.: Recent advances in surrogate-based optimization. *Prog. Aerosp. Sci.* 45(1), 50–79 (2009). <http://www.sciencedirect.com/science/article/pii/S0376042108000766>
- Dubourg, V., et al.: Metamodel-based importance sampling for structural reliability analysis. *Probabilistic Eng. Mech.* 33, 47–57 (2013)
- Zhu, P., et al.: A novel machine learning model for eddy current testing with uncertainty. *NDT & E Int.* 101, 104–112 (2019)

29. Bishop, C.M.: *Pattern Recognition and Machine Learning* (Information Science and Statistics). Springer-Verlag, New York (2006)
30. Cristianini, J.S.T.N.: *Kernel Methods for Pattern Analysis*. Cambridge University Press, Cambridge (2004)
31. Smola, A.J., Schölkopf, B.: *Sparse Greedy Matrix Approximation for Machine Learning*, pp. 911–918. Morgan Kaufmann, San Francisco (2000)
32. Forrester, A.I.J., et al.: *Engineering Design via Surrogate Modelling - A Practical Guide*. Wiley, Chichester (2008)
33. Crombecq, K., et al.: Efficient space-filling and non-collapsing sequential design strategies for simulation-based modeling. *Eur. J. Oper. Res.* 214(3), 683–696 (2011)
34. Miorelli, R., et al.: A machine learning approach for classification tasks of ECT signals in steam generator tubes nearby support plate. *AIP Conf. Proc.* 2102(1), 090004 (2019)
35. Salucci, M., et al.: A nonlinear kernel-based adaptive learning-by-examples method for robust NDT/NDE of conductive tubes. *J. Electromagn. Waves Appl.* 33(6), 669–696 (2019)

How to cite this article: Miorelli R, Skarlatos A, Reboud C. Flaw characterization in conductive media based on pulsed Eddy current measurements: A fast non-iterative inversion approach. *IET Sci Meas Technol.* 2021;15:259–267. <https://doi.org/10.1049/smt2.12027>